Turk J Elec Eng & Comp Sci, Vol.19, No.4, 2011, © TÜBİTAK
doi:10.3906/elk-0808-22

Decentralized robust load-frequency control of power system based on quantitative feedback theory

Aidin SAKHAVATI[1,*], **Gevork B. GHAREHPETIAN**[2], **Seyed Hossein HOSSEINI**[3]
[1] *Department of Electrical Engineering, Science and Research Branch, Islamic Azad University, (IAU), Tehran-IRAN*
e-mail: aidin_sakhavati@yahoo.com
[2] *Electrical Engineering Department, Amirkabir University of Technology Tehran-IRAN*
e-mail: grptian@aut.ac.ir
[3] *Faculty of Electrical and Computer Engineering, University of Tabriz, Tabriz-IRAN*
e-mail: hosseini@tabrizu.ac.ir

Received: 21.08.2008

Abstract

This paper aims at investigating the problem of Load Frequency Control (LFC) in interconnected power systems in order to obtain robustness against uncertainties. A design method for a robust controller, based on Quantitative Feedback Theory (QFT), has been presented in this paper. For a two-area power system, the simulation results show that the system response with the proposed QFT controller exhibits transient response beyond PI controllers. It is also shown that the transient response of the tie line power can also be improved.

Key Words: *Load frequency control, power system control, quantitative feedback theory, robust control*

1. Introduction

Load Frequency Control (LFC) is one of the most important issues in power system control and design. LFC is used to maintain the system frequency and the inter-area tie-line power close to the scheduled values [1]. Design of LFC is conventionally based on linear model with fixed system parameters. An optimal control theory has been proposed in [2] and utilized since the early 1970s. Fuzzy logic-based extended Proportional Integral (PI) controller for LFC has been suggested in [3, 4]. These methods improve the dynamic performance of the power system in comparison with the conventional PI controller. The methods are based on the decentralized design with nominal plant parameters. Therefore, they cannot be directly applied to the interconnected power systems with uncertainties. Thus, the important criteria in the design of LFC should inevitably include parameter perturbation. Most physical plants are often modeled approximately based on the linearization around operating point and may be subjected to the plant parameter variation. LFC design based on the nominal system parameters is unable to guarantee both stability and the desired performance of the power

*Corresponding author: Department of Electrical Engineering, Science and Research Branch, Islamic Azad University (IAU), Tehran-IRAN

system with parametric uncertainties. Therefore, modern control methods such as adaptive control method have already been used [5–8]. These methods, however, require either information on the system states or an efficient on-line identifier. Model reference adaptive methods also require satisfying the prefect model to follow conditions and the complete system state information. Since the order of the power system is high, the model reference approach may be difficult to be applied. Other various methods such as variable structure control [9] and robust control [10–15] have been used to design LFC. In power system control, it is desirable to design the controllers, which achieve robust stability due to parametric uncertainties.

One can consider a control based on Quantitative Feedback Theory (QFT) as a system offering robustness against signal uncertainty and as a natural extension of classical frequency domain design approaches [16]. The design of a proportional–integral–derivative (PID) controller for LFC of a unified (centralized) power system, based on maximum peak-resonance specification and QFT methods, has been proposed by [17] and [18]. It must be noted that QFT was initially proposed by Horowitz and further developed by others [19]. It is considered as an efficient method for designing the robust controllers for plants with parameter uncertainties, unstructured uncertainties and mixed uncertainties, and has been applied the flight control, missile control, compact disk mechanism, etc. [16, 20]. This method was first proposed for minimum-phase and stable systems. Chen and others then developed this method even for uncertain non-minimum phase and unstable plants [21].

In QFT one of the main objectives is to design a simple, low order controller with minimum bandwidth. The minimum bandwidth controllers are natural requirements in practice, in order to avoid problems with noise amplification, resonances and un-modeled high frequency dynamics. In most practical design situations, iterations are inevitable and QFT offers direct insight into the available trade-off between controller complexity and specifications during such iterations.

This paper proposes a decentralized robust LFC controller based on QFT. The simulation results, carried out by MATLAB Simulink toolbox, show that the proposed controllers guarantee the robust performance of the plant for a wide range of operating conditions. To indicate the effectiveness of proposed technique, this method has been compared with a PI controller optimized by Genetic Algorithm or Particle Swarm Optimization. Both, the proposed and classical methods are applied to a two-area power system. The results of simulations show that the QFT controllers guarantee the robust performance and better dynamic response, such as minimum overshoot and settling time in comparison with the classical controllers such as PI-PSO or PI-GA, considering uncertainties in system parameters. Also, it is shown that the tie-line power flow oscillations can be damped by the proposed controller.

In this paper, a dynamical model of each control area for the load frequency control problem is presented in section 2. Next, the robust control design, which is based on QFT method, is described in section 3. In section 4, the proposed controller is tested on a given two-area power system and its performance is compared with that of a conventional controller.

2. Power system model

2.1. State equations

An interconnected electric power system can be considered as control areas connected with tie lines. There are various complicated nonlinear models for large power systems. However, usually linearized model has been used [1]. In this paper, a two-area power system, shown in Figure 1, has been studied and the errors of the linearization have been considered as parametric uncertainties and un-modeled dynamics.

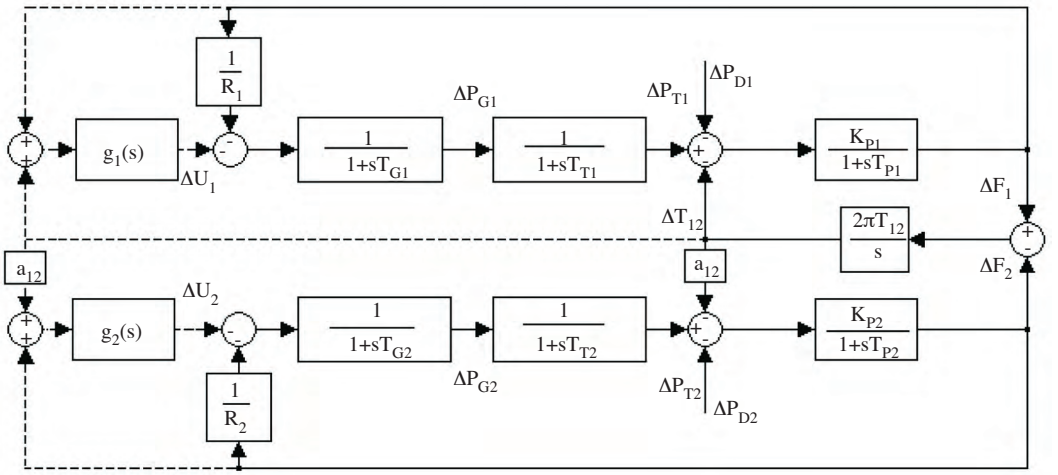

Figure 1. Block diagram of two-area power system.

Each area consists of three first-order transfer functions, modeling the system turbine, governor and power system. In addition, all generators in each area have been assumed to form a coherent group. The state space model of the two-area power system can be presented by the relations

$$\begin{cases} \dot{\mathbf{x}} = \mathbf{A}\mathbf{x} + \mathbf{B}\mathbf{u} + \mathbf{F}\mathbf{d} \\ \mathbf{y} = \mathbf{C}\mathbf{x}, \end{cases} \tag{1}$$

where $\mathbf{x}$ is the state variables vector, $\mathbf{y}$ is the output vector, $\mathbf{u}$ is control signals and $\mathbf{d}$ is the input vector, as follows:

$$\mathbf{x} = \begin{bmatrix} \Delta P_{T1} & \Delta P_{G1} & \Delta F_1 & \Delta T_{12} & \Delta P_{T2} & \Delta P_{G2} & \Delta F_2 \end{bmatrix}^T,$$

$$\mathbf{d} = \begin{bmatrix} \Delta P_{D1} & \Delta\ P_{D2} \end{bmatrix}^T,$$

$$\mathbf{y} = \begin{bmatrix} \Delta F_1 & \Delta F_2 \end{bmatrix}^T,$$

$$\mathbf{u} = \begin{bmatrix} \Delta u_1 & \Delta u_2 \end{bmatrix}^T.$$

We also have

$$\mathbf{A} = \begin{bmatrix} -1/T_{T1} & 1/T_{T1} & 0 & 0 & 0 & 0 & 0 \\ 0 & -1/T_{G1} & -1/(R_1 T_{G1}) & 0 & 0 & 0 & 0 \\ K_{P1}/T_{P1} & 0 & -1/T_{P1} & K_{P1}/T_{P1} & 0 & 0 & 0 \\ 0 & 0 & 2\pi T_{12} & 0 & 0 & 0 & -2\pi T_{12} \\ 0 & 0 & 0 & 0 & -1/T_{T2} & 1/T_{T2} & 0 \\ 0 & 0 & 0 & 0 & 0 & -1/T_{G2} & -1/(R_2 T_{G2}) \\ 0 & 0 & 0 & K_{P2}/T_{P2} & K_{P2}/T_{P2} & 0 & -1/T_{P2} \end{bmatrix},$$

$$\mathbf{B} = \begin{bmatrix} 0 & 1/T_{G1} & 0 & 0 & 0 & 0 & 0 \\ 0 & 0 & 0 & 0 & 0 & 1/T_{G2} & 0 \end{bmatrix}^T,$$

$$\mathbf{F} = \begin{bmatrix} 0 & 0 & -K_{P1}/T_{P1} & 0 & 0 & 0 & 0 \\ 0 & 0 & 0 & 0 & 0 & 0 & -K_{P2}/T_{P2} \end{bmatrix}^T,$$

$$\mathbf{C} = \begin{bmatrix} 0 & 0 & 1 & 0 & 0 & 0 & 0 \\ 0 & 0 & 0 & 0 & 0 & 0 & 1 \end{bmatrix}.$$

The elements of the above mentioned matrices and vectors have been presented in appendix A.

3. Parametric uncertainty

In Figure 1, there is one robust controller for each area of the power system. The operating points of the power system may randomly change during a daily cycle due to the inherent characteristics of load variation and system configuration. As a result, the parametric uncertainties of the power system should be considered. Table 1 shows the six parametric uncertainties of the power system with their nominal and the lower and upper bound values. In Table 1, P_{Ui} and P_{Li} denote the upper and lower bound values, respectively, and $P_{i\ nom}$ is the nominal value of the parameter. In [22], the system parametric uncertainties are obtained by changing parameters by 30% to 50% from their typical values; so, in this paper, the range of parameter variations can be calculated by changing the nominal values of T_{Pi}, K_{pi}, T_{12}, R_i , T_{Ti} and T_{Gi} in the range of $\pm 50\%$ of their typical values given in Appendix B.

Table 1. Parametric uncertainties of power system.

P_i	P_{Li}	$P_{i\ nom}$	$\boldsymbol{P}_{Ui}$
K_{Pi}	60	120	180
T_{Pi}	10	20	30
T_{12}	0.0433	0.0866	0.1299
R_i	1.2	2.4	3.6
T_{Ti}	0.15	0.3	0.45
$\boldsymbol{T}_{Gi}$	0.04	0.08	0.12

4. Design of LFC using QFT

4.1. Performance specifications and assumptions

The designed LFC controller should guarantee some of the important performance specifications, including:

a. Power system stability within variations of operating point.

b. Acceptable dynamic response for step changes in load, such as minimum peak response.

c. Frequency and tie-line power variations should be equal to zero in steady state.

In QFT, the closed-loop transfer function should satisfy certain performance requirements for a set of discrete frequencies. These requirements are specified in terms of tolerance bands within which the magnitude response of the closed-loop transfer function should be limited. The uncertainties in the plant are transformed onto the Nichols chart resulting in bounds on the open loop transfer function of the system. A compensator is then chosen by manually shaping the loop transmission so that it satisfies the bounds at each of the frequency points. A pre-filter is then used to ensure that the closed-loop transfer function lies within the specified bands. The feedback system of two-area power system is shown schematically in Figure 2. In the figure, blocks and

paths marked **F**, **G**, **P**, **r**, **d** and **y** denote the pre-filter, controller, plant, reference input, disturbance and output of the system, respectively. To design a robust LFC based on QFT, the following assumptions have been considered:

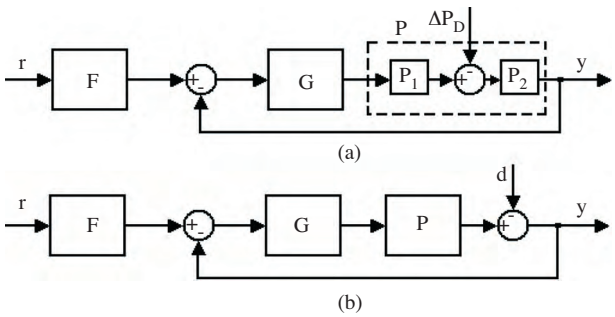

Figure 2. MIMO system with disturbances (a) in a real situation and (b) at plant's output.

(a) The load, machine, turbine and governor transfer function is supposed to be as **P** (plant dynamics), as shown in Figure 2(a). Here, P_1 is the turbine and governor and P_2 is the load and machine transfer functions. Therefore, ΔP_{Di} will be disturbances at the middle of plant **P** (neither before nor after), as shown in Figure 2(a). The design procedure needs the change of ΔP_{Di} to the plant output, as shown in Figure 2(b). According to Figure 3, $\Delta P'_{\mathrm{Di}}$ can be used instead of ΔP_D. As a result, $\Delta P'_{\mathrm{Di}}$is used as output disturbances.

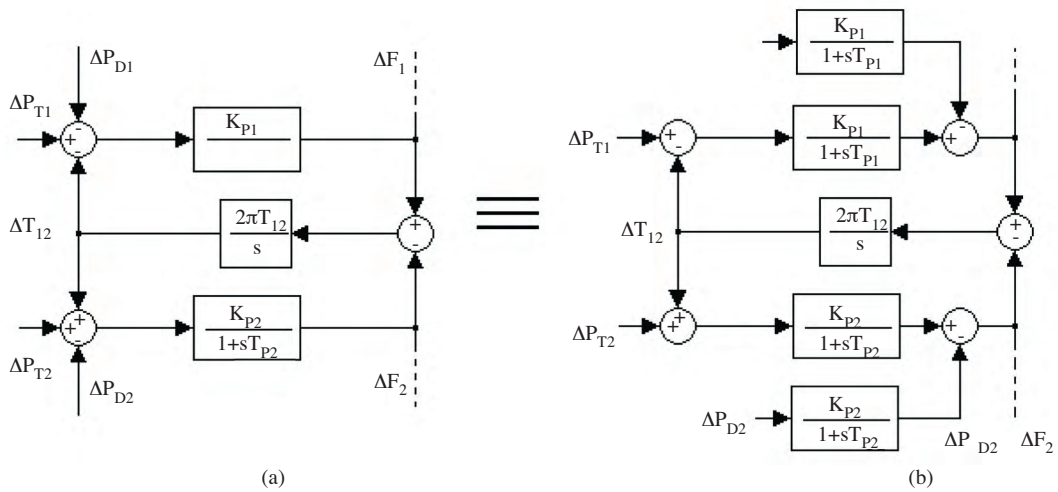

Figure 3. (a) ΔP_{Di} as disturbances in a real situation; and (b)$\Delta P'_{\mathrm{D}i}$ as disturbances in plant's output.

(b) ΔP_{ref} is the reference signal. The effect of ΔP_{ref} in LFC is not considered. Therefore the design of the pre-filter is ignored.

(c) The poles and zeros of the controller **G** shown in Figure 2, are designed using QFT toolbox in MATLAB [16] with some modifications, so that the open-loop transfer function is reshaped.

4.2. QFT design

The problem is how to compute bounds on the controller $\mathbf{G}$. The given margin specifications will be satisfied for the plant $\mathbf{P}(s)$:

$$\mathbf{P}(s) = \begin{bmatrix} p_{11}(s) & p_{12}(s) \\ p_{21}(s) & p_{22}(s) \end{bmatrix}. \tag{2}$$

It must be noted that for the different operating points, we have a set of plants. During the design procedure these bounds will intersect the generated bounds to satisfy other specifications. The result will also satisfy the margin specifications. The MIMO (Multi-Input Multi-Output) QFT sequential design procedure considers diagonal controllers, i.e. $\mathbf{G}(s)$, as

$$\mathbf{G}(s) = \begin{bmatrix} g_1(s) & 0 \\ 0 & g_2(s) \end{bmatrix}. \tag{3}$$

The sequential procedure involves a sequential single-loop design of each loop of the system. The robust stability of MIMO system is related to the stability of MIMO characteristics equation:

$$\det(\mathbf{I} + \mathbf{PG}) = (1 + p_{11}g_1)(1 + p_{22}^{eq}g_2) = 0, \tag{4}$$

where

$$p_{22}^{eq} = p_{22} - \frac{p_{12}p_{21}g_1}{1 + p_{11}g_1}. \tag{5}$$

Then, the MIMO system is robust stable, if each of the two functions on the right-hand side of the equation (4) is robust stable. The diagonal controller, $\mathbf{G}(s)$ is designed to satisfy the performance specifications: a. Robust stability, b. Robust margins, and c. Robust sensitivity rejection.

For robust margins (via closed-loop magnitude peaks) specification, we have:

$$\frac{1}{|1 + L_i(j\omega)|}\langle 1.2 \quad \omega\rangle 0, \quad i = 1, 2. \tag{6}$$

According to Figure 4, the transfer function of $\frac{y_1}{r_1}$, L_1, for when K_1 is open and K_2 is closed, is

$$L_1 = g_1p_{11} - \frac{g_1g_2p_{12}p_{21}}{1 + g_2p_{22}}. \tag{7}$$

In the same way, L_2 can be

$$L_2 = g_2p_{22} - \frac{g_1g_2p_{12}p_{21}}{1 + p_{11}g_1}. \tag{8}$$

For the robust sensitivity rejection specification [23], we have

$$\begin{aligned} &[\mathbf{S_{ij}}] = (\mathbf{I} + \mathbf{PG})^{-1} = \left(\begin{bmatrix} 1 & 0 \\ 0 & 1 \end{bmatrix} + \begin{bmatrix} p_{11} & p_{12} \\ p_{21} & p_{22} \end{bmatrix} \begin{bmatrix} g_1 & 0 \\ 0 & g_2 \end{bmatrix} \right)^{-1} \text{ and} \\ &|\mathbf{S_{ij}}(j\omega)| \leq \eta_{ij} \qquad \omega < 100 \end{aligned} \tag{9}$$

where

$$\eta_{ij} = \begin{cases} 0.01\omega & i = j \\ 0.005\omega & i \neq j. \end{cases}$$

Considering equations (7) and (8), we have

$$L_1 = g_1 \frac{p_{11} + g_2 \det \mathbf{P}}{1 + g_2 p_{22}} \tag{10}$$

$$L_2 = g_2 \frac{p_{22} + g_1 \det \mathbf{P}}{1 + g_1 p_{11}} \tag{11}$$

where

$$\det \mathbf{P} = (p_{11}p_{22} - p_{12}p_{21}). \tag{12}$$

In this paper, the design procedure proceeds in two stages. Considering equations (6) and (10), the margin condition on $L_1(j\omega)$ for the first stage of the g_1 design can be described by the equation

$$\left| \frac{1 + g_1 p_{11} + g_2(p_{22} + g_1 \det \mathbf{P})}{1 + g_2 p_{22}} \right|^{-1} \equiv \left| \frac{A + g_2 B}{C + g_2 D} \right|^{-1} \leq 1.2. \tag{13}$$

It is assumed g_1 is known. A solution of $g_L \leq |g_2(j\omega)| \leq g_U$ is usually unacceptable, as it may result in an empty region for g_2 when intersected with other bounds [23]. If an acceptable solution exists, it is typically in the form of $|g_2(j\omega)| \geq g_U$ or $|g_2(j\omega)| \leq g_L$. Therefore, a necessary condition for the existence of a finite bandwidth solution is $g_L > 0$ at high frequencies and a necessary condition on the bounds of $g_2\ (j\omega)$, so that $g_2(j\omega)$ has a finite bandwidth solution, is the existence of an ω_{mb}, as follows:

$$\lim_{|g_2| \to \infty} |1 + L_1|^{-1} = \left| 1 + g_1 \frac{\det \mathbf{P}}{p_{22}} \right|^{-1} \leq 1.2. \tag{14}$$

$$\lim_{|g_2| \to 0} |1 + L_1|^{-1} = |1 + g_1 p_{11}|^{-1} \leq 1.2. \tag{15}$$

On the other hand, the robust sensitivity rejection for the first stage of g_1 design, considering the equation (9), can be described by the equations

$$|S_{11}(j\omega)| = \left| \frac{1 + p_{22}g_2}{(1 + p_{11}g_1)(1 + p_{22}g_2) - p_{12}p_{21}g_1g_2} \right| \leq \eta_{11}, \tag{16}$$

$$|S_{12}(j\omega)| = \left| \frac{-p_{12}g_2}{(1 + p_{11}g_1)(1 + p_{22}g_2) - p_{12}p_{21}g_1g_2} \right| \leq \eta_{12}, \tag{17}$$

where g_2, at this stage, is unknown. As a result, equations (16) and (17) should be rewritten by using the equation presented in Appendix C as follows:

$$|S_{11}(j\omega)| = \left| \frac{p_{22} - p_{12}S_{21}}{p_{22} + g_1 \det \mathbf{P}} \right| \leq \eta_{11}, \tag{18}$$

$$|S_{12}(j\omega)| = \left| \frac{-p_{12} + p_{12}S_{22}}{p_{22} + g_1 \det \mathbf{P}} \right| \leq \eta_{12}. \tag{19}$$

With $|S_{21}| \leq \eta_{21}$ and $|S_{22}| \leq \eta_{22}$, the equations (18) and (19) can be rewritten as

$$\left| \frac{|p_{22}| + |p_{12}|\,\eta_{21}}{p_{22} + g_1 \det \mathbf{P}} \right| \leq \eta_{11}, \tag{20}$$

$$\left| \frac{|p_{12}| + |p_{12}|\,\eta_{22}}{p_{22} + g_1 \det \mathbf{P}} \right| \leq \eta_{12}. \tag{21}$$

In this two-stage sequential procedure, in the first stage, g_1 is designed to satisfy calculated bounds and to meet other specifications (equations (14), (15), (20) and (21)).

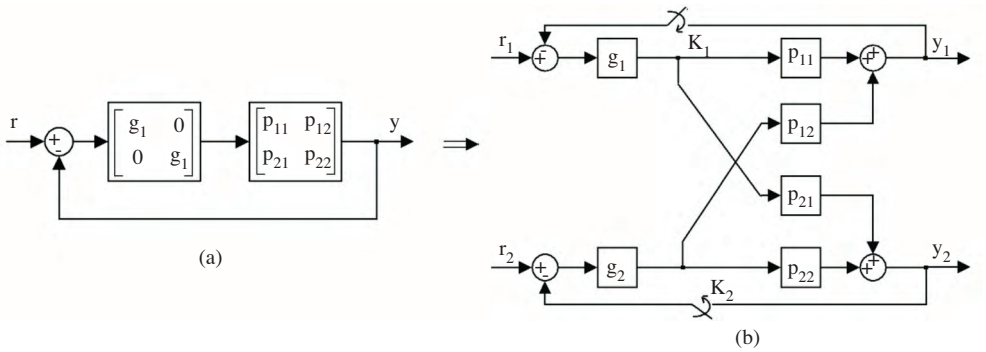

Figure 4. Expanded 2-input 2-output power system.

In the second stage, g_2 is designed to satisfy calculated bounds once again and to meet the specifications, considering the following equations:

$$|1 + L_1|^{-1} = \left| 1 + g_1 \frac{p_{11} + g_2 \det \mathbf{P}}{1 + g_2 p_{22}} \right|^{-1} \leq 1.2, \tag{22}$$

$$|1 + L_2|^{-1} = \left| 1 + g_2 \frac{p_{22} + g_1 \det \mathbf{P}}{1 + g_1 p_{11}} \right|^{-1} \leq 1.2. \tag{23}$$

Also, the robust sensitivity rejection for second stage design g_2 is in the form

$$|S_{21}(j\omega)| = \left| \frac{1 + p_{11} g_1}{(1 + p_{11} g_1)(1 + p_{22} g_2) - p_{12} p_{21} g_1 g_2} \right| \leq \eta_{21}, \tag{24}$$

$$|S_{22}(j\omega)| = \left| \frac{-p_{21} g_1}{(1 + p_{11} g_1)(1 + p_{22} g_2) - p_{12} p_{21} g_1 g_2} \right| \leq \eta_{22}. \tag{25}$$

One of the most important objectives in control design is to use an accurate description of plant dynamics. The QFT and its design procedure requires one to define the plant dynamics only in frequency domain. The term template is then used to denote the collection of an uncertain plant's frequency responses at a given frequency. The frequency range must be chosen based on the performance bandwidth and the shape of the templates. Margin bounds should be calculated up to the frequency where the shape of the plant template becomes invariant to frequency. For the power system, studied in this paper, the template shape becomes a vertical fixed line at $\omega = 500$ rad/sec. The plant templates at several frequencies are shown in Figures 5(a) and 5(b), for plants p_{11} (or p_{22}) and p_{12} (or p_{21}), respectively. It must be noted that the plant parameters of each area is assumed to be equal, as a result, $p_{11} = p_{22}$ and $p_{12} = p_{21}$.

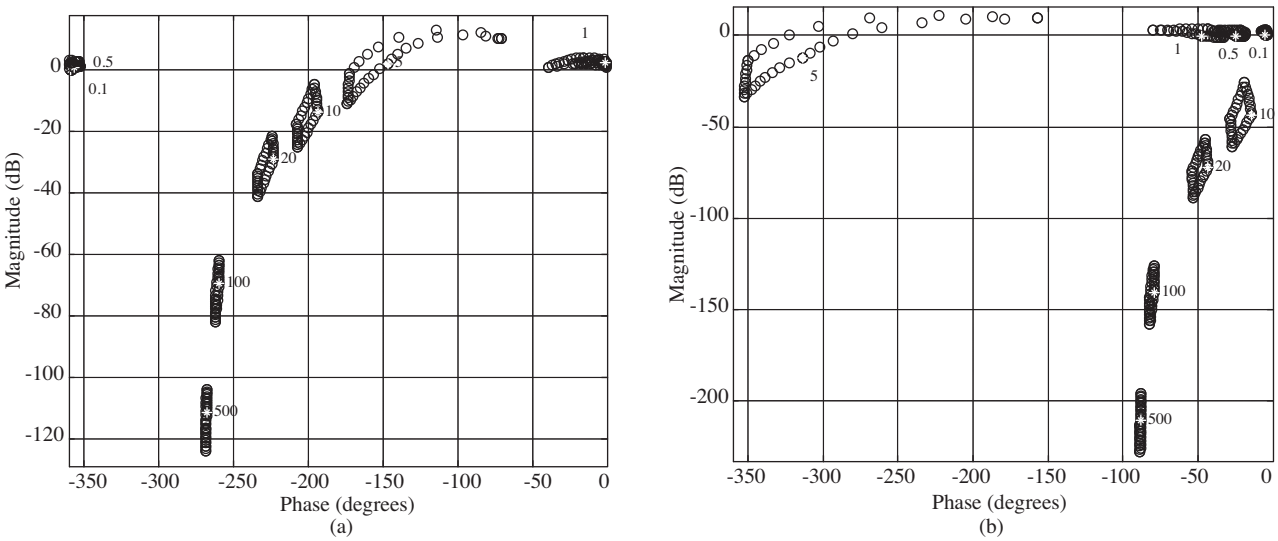

Figure 5. Plant templates for (a) p_{11} or p_{22} (b) p_{12} or p_{21}.

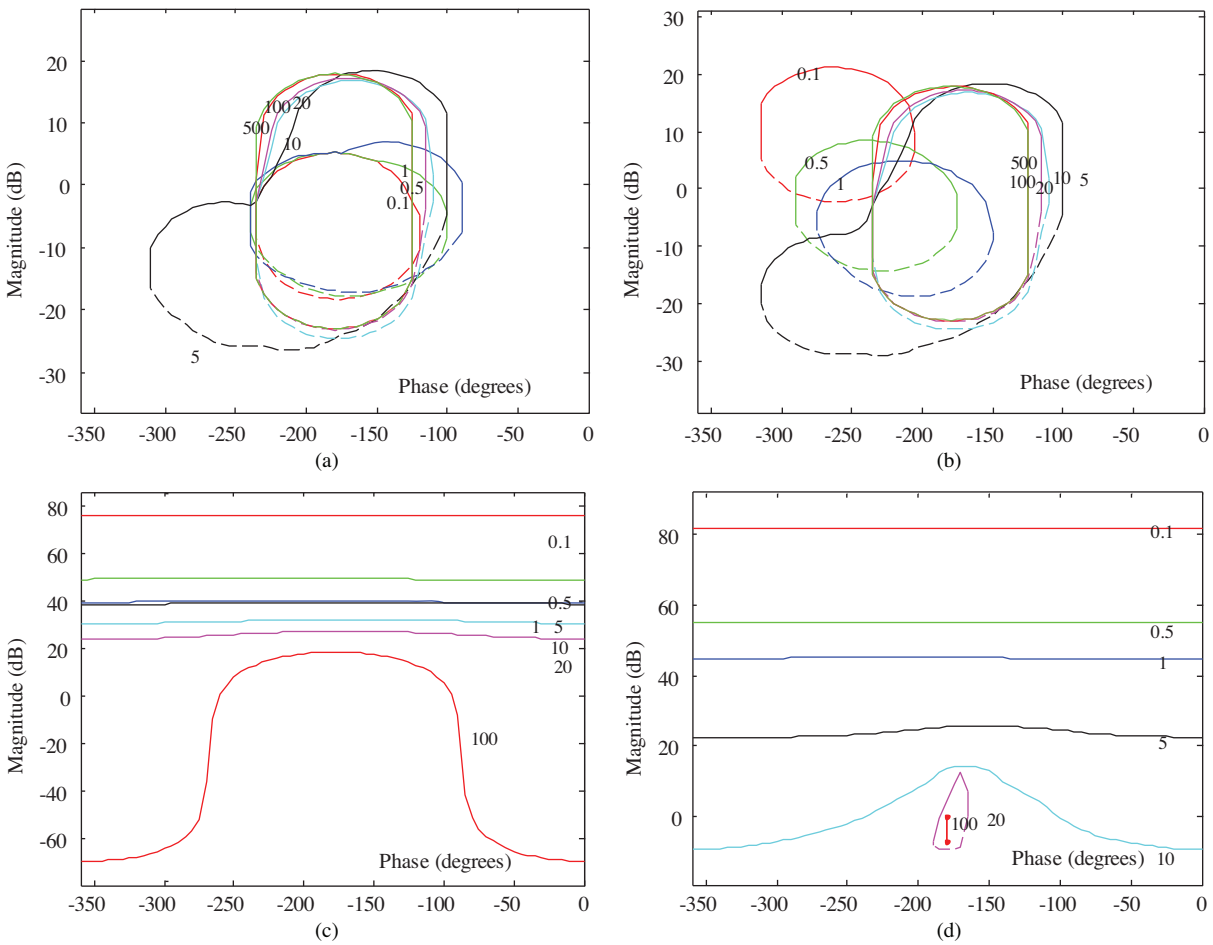

Figure 6. g_1 robust margin bounds: (a) $g_2 \to \infty$, (b) $g_2 = 0$ and robust sensitivity rejection bounds (c) $|S_{11}(j\omega)| \leq \eta_{11}$ and (d) $|S_{12}(j\omega)| \leq \eta_{12}$.

In the first design stage, the calculated bounds (according to Equations (14), (15), (20) and (21)) are shown in Figures 6(a)–6(d), respectively. The intersection of these bounds is shown in the Figure 7(a). Also, the Figure 7(a) includes the loop $L_1 = g_1 p_{11}$ for the nominal plant case. So, the controller g_1 is

$$g_1 = \frac{L_1}{p_{11}}. \tag{26}$$

In the second design stage, the calculated bounds (according to Equations (22)–(25)) are shown in Figure 7(b). It must be noted that, in this stage, g_1 has been determined by the equation (26). The Figure 7(b) presents the nominal second loop $L_2 = g_2 p_{22}^{eq}$, thus the second controller g_2 can be calculated by the equation

$$g_2 = \frac{L_2}{p_{22}^{eq}}. \tag{27}$$

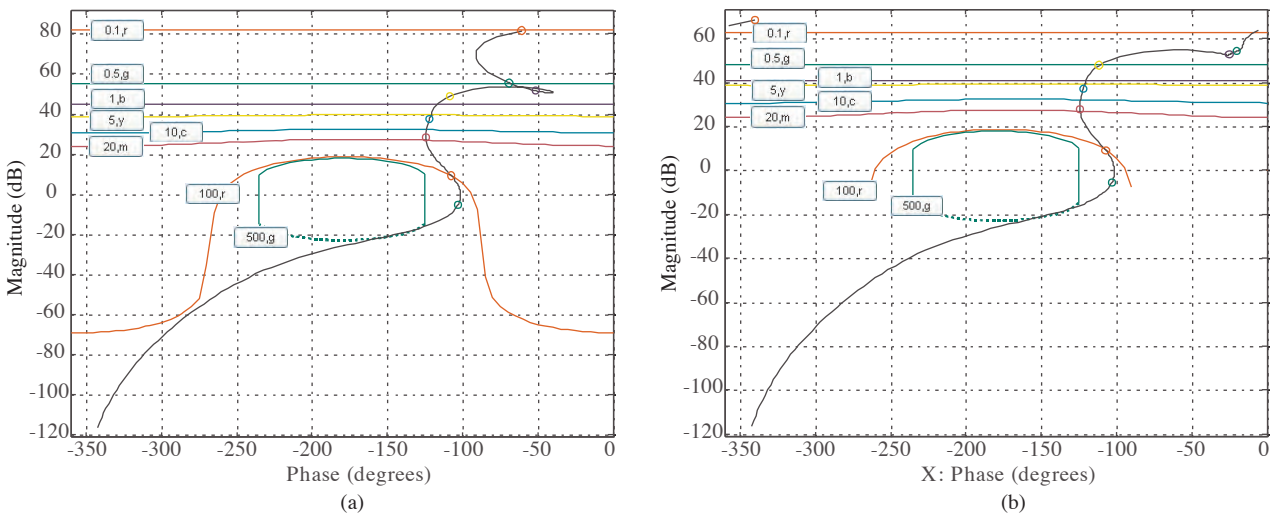

Figure 7. Intersection of all bounds with loop shaping for (a) first loop and (b) second loop.

The parameters of two areas are the same. As a result, controllers g_1 and g_2 should be the same:

$$g_1 = g_2 = \frac{14.3(s/42.6+1)(s/3.3+1)(s/2.2+1)(s/0.04+1)(s/0.01+1)}{(s/2500+1)(s^2/0.008+s/0.47+1)(s^2/2.3\times 10^{-7}+s/3427+1)}$$

The loop-shaping programming and QFT toolbox of Matlab [16] was used to design the loop-shape shown in Figure 7. Now, the frequency response of robust margin conditions can be determined by equation (6) and it is shown in Figure 8(a). It can be seen that the robust margin conditions are guaranteed at all frequencies. Also, the frequency response of robust sensitivity rejection (equation 9) is shown in Figure 8(b). The robust sensitivity rejection of the system is guaranteed, too.

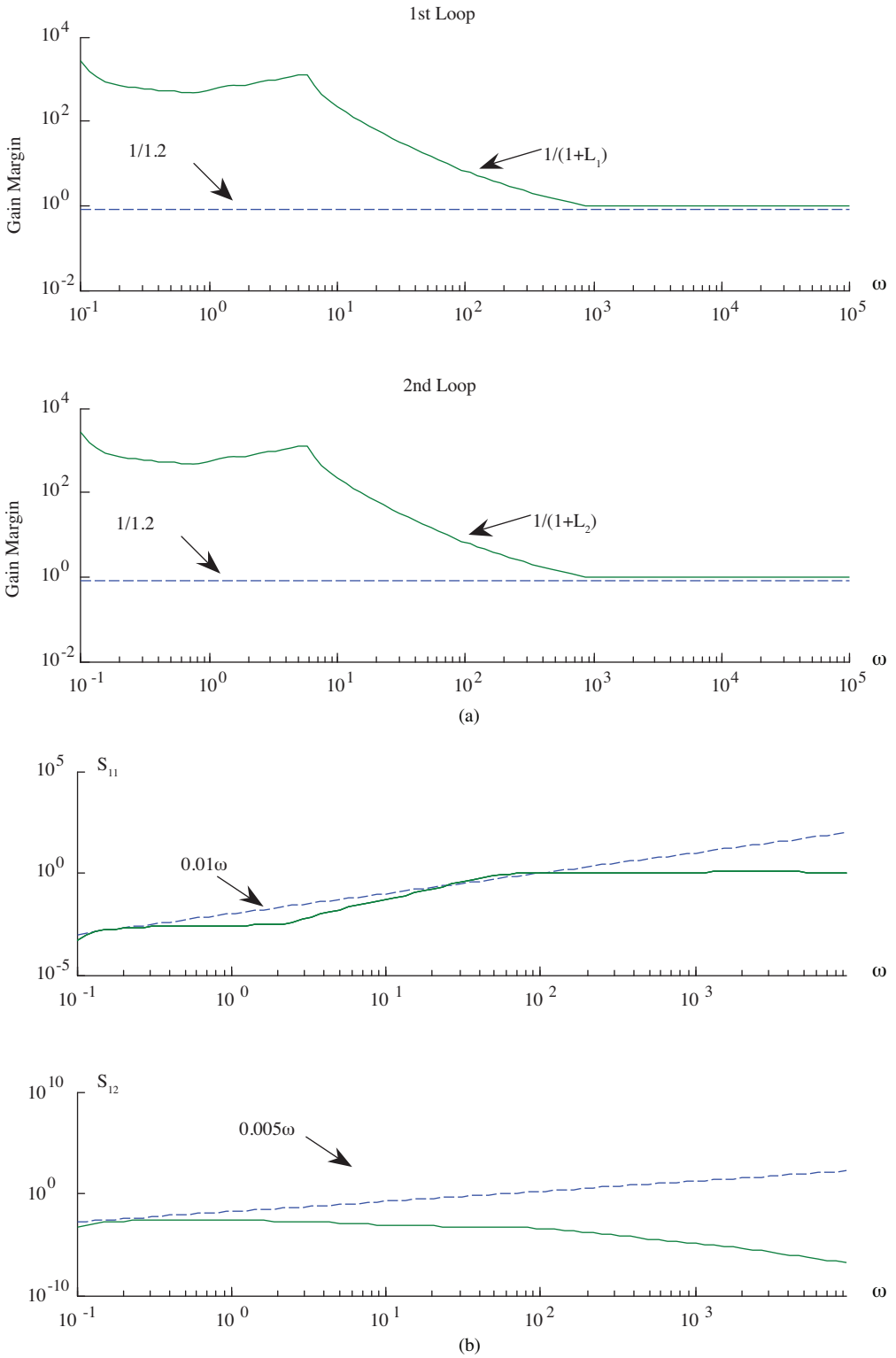

Figure 8. Frequency response of (a) robust margin conditions for 1^{st} loop and 2^{nd} loop (b) robust sensitivity rejection.

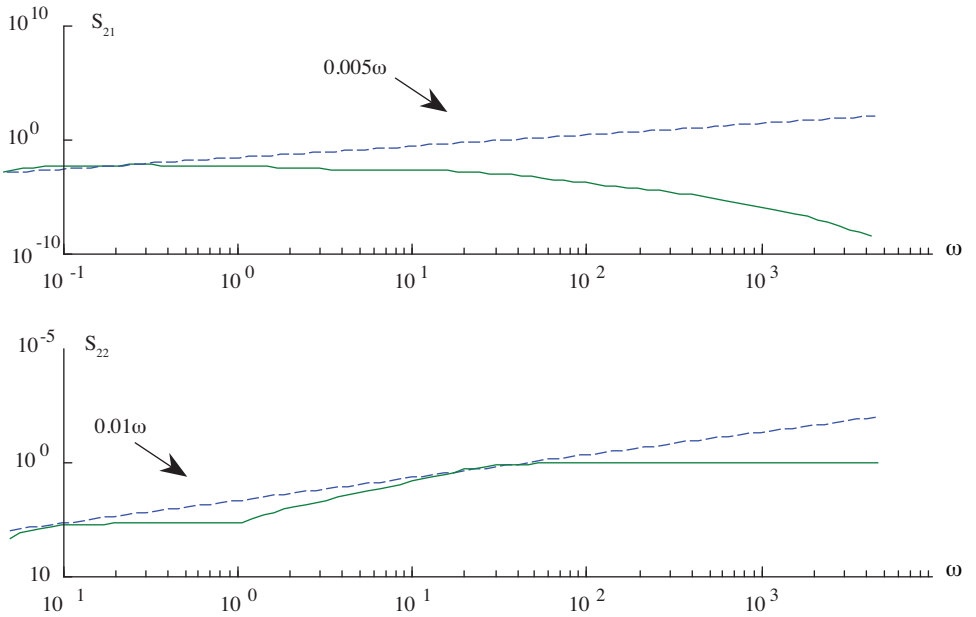

Figure 8. Contunied.

5. Simulation results

The two-area power system shown in Figure 1, with the parameters given in appendix A, and nominal values given in appendix B, has been simulated. The simulated system is controlled by:

A: Genetic Algorithm (GA) [24, 25] and Particle Swarm Optimization (PSO) [26] based designed conventional PI; and

B: QFT based designed robust controllers.

The nine operating points of the system have been given in Table 2. For these 9 operating points, Figures 9 and 10 depict the frequency change and the tie line power deviations for a 2% load step change in the first area with a PI-GA (or PI-PSO) and QFT controllers, respectively. In Figure 11, the frequency and the tie line power deviations are compared in the nominal case. It can be seen that the response of QFT controller are better than the conventional GA-PI (or PSO-PI) controllers. Also, Figures 9 and 10 show that the system response to the proposed QFT controller has a better transient response than the response of the PI controllers. Besides,

Table 2. Nine operating points of power system.

Operating points	K_{P1}	K_{P2}	T_{P1}	T_{P2}	R_1	R_2	T_{T1}	T_{T2}	T_{G1}	T_{G2}	T_{12}
a	120	120	20	20	2.4	2.4	0.3	0.3	0.08	0.08	0.0866
b	180	120	30	20	3.6	2.4	0.45	0.3	0.12	0.08	0.0866
c	60	120	10	20	1.2	2.4	0.15	0.3	0.04	0.08	0.0866
d	180	60	30	10	3.6	1.2	0.45	0.15	0.12	0.04	0.0433
e	180	60	30	10	3.6	1.2	0.45	0.15	0.12	0.04	0.1299
f	180	180	10	10	1.2	1.2	0.15	0.15	0.04	0.04	0.0433
g	60	60	10	10	1.2	1.2	0.15	0.15	0.04	0.04	0.0433
h	60	60	30	30	3.6	3.6	0.45	0.45	0.12	0.12	0.0433
i	60	60	30	30	3.6	3.6	0.45	0.45	0.12	0.12	0.0866

it also verifies that the transient response of the tie line power flow has been improved, too. Also, Figure 10 shows that the proposed QFT controller presents the robust performance considering parametric uncertainties. As it can be seen in Figure 9 (a), the operating points (h) and (i) are unstable in the case of using PI controller. But, according to Figure 10 (a), these operating points are stable in the case of using proposed controller. Therefore, it can be said that the proposed robust controller can improve the system dynamic performance and the stability, too.

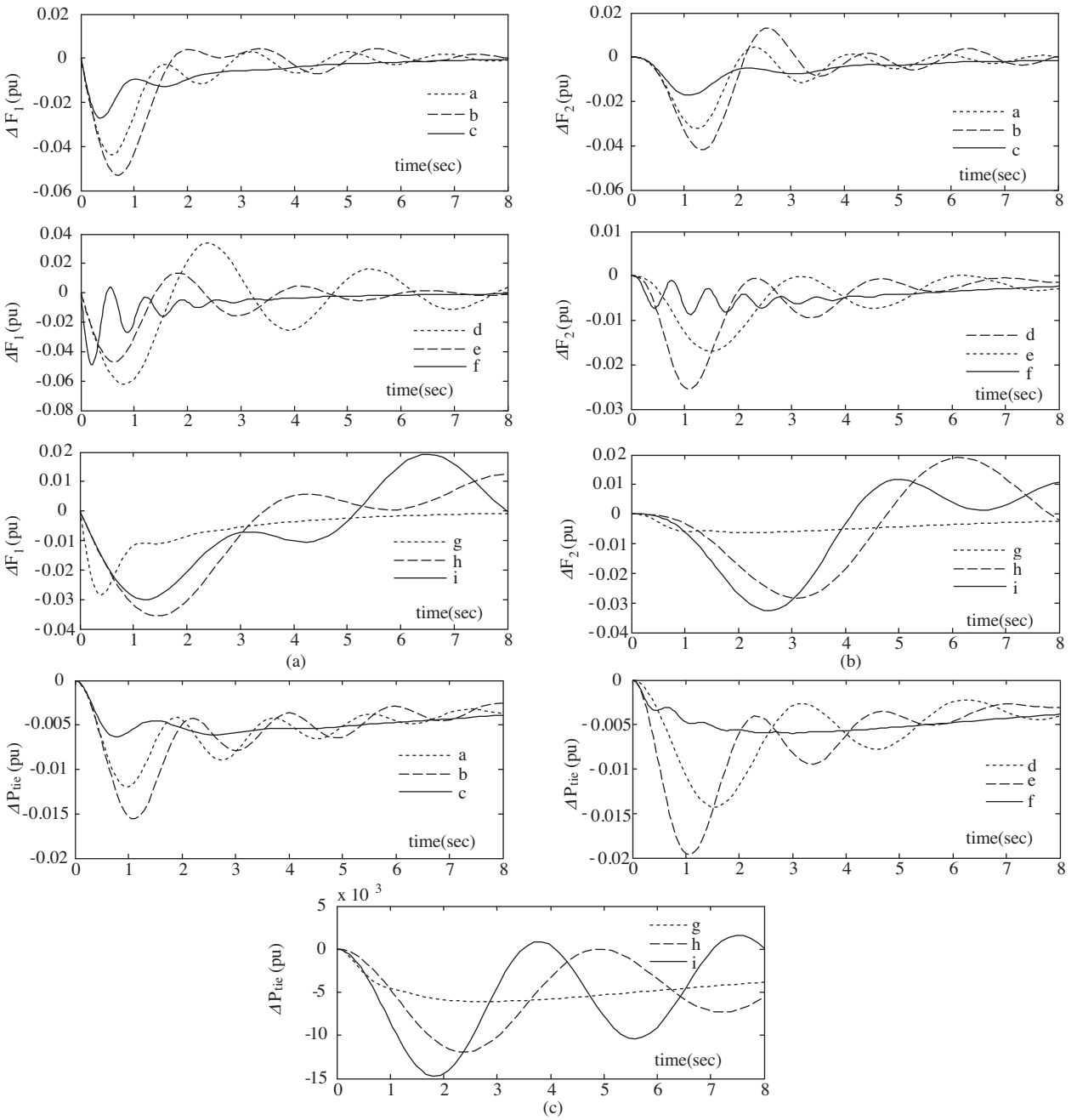

Figure 9. Frequency and tie line power deviations: (a) $\Delta F_1(t)$, (b) $\Delta F_2(t)$, and (c) ΔP_{tie}(t) for nine operating points for a 2% load step change in first area with a PI controller (results of PI-GA and PI-PSO are the same).

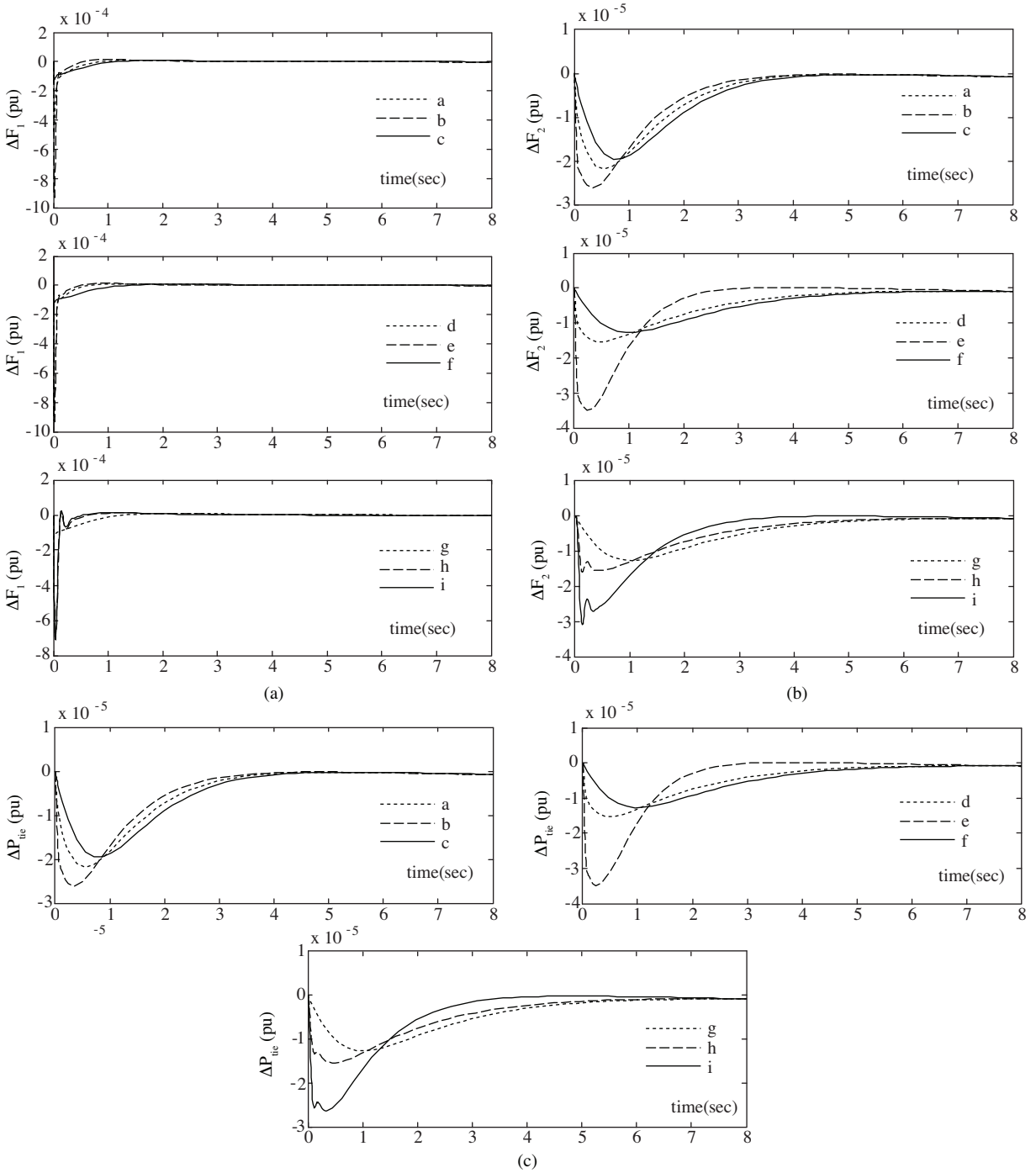

Figure 10. Frequency and tie line power deviations: (a) $\Delta F_1(t)$, (b) $\Delta F_2(t)$, and (c) $\Delta P_{tie}(t)$ for 9 operating points for a 2% load step change in first area with a QFT controller.

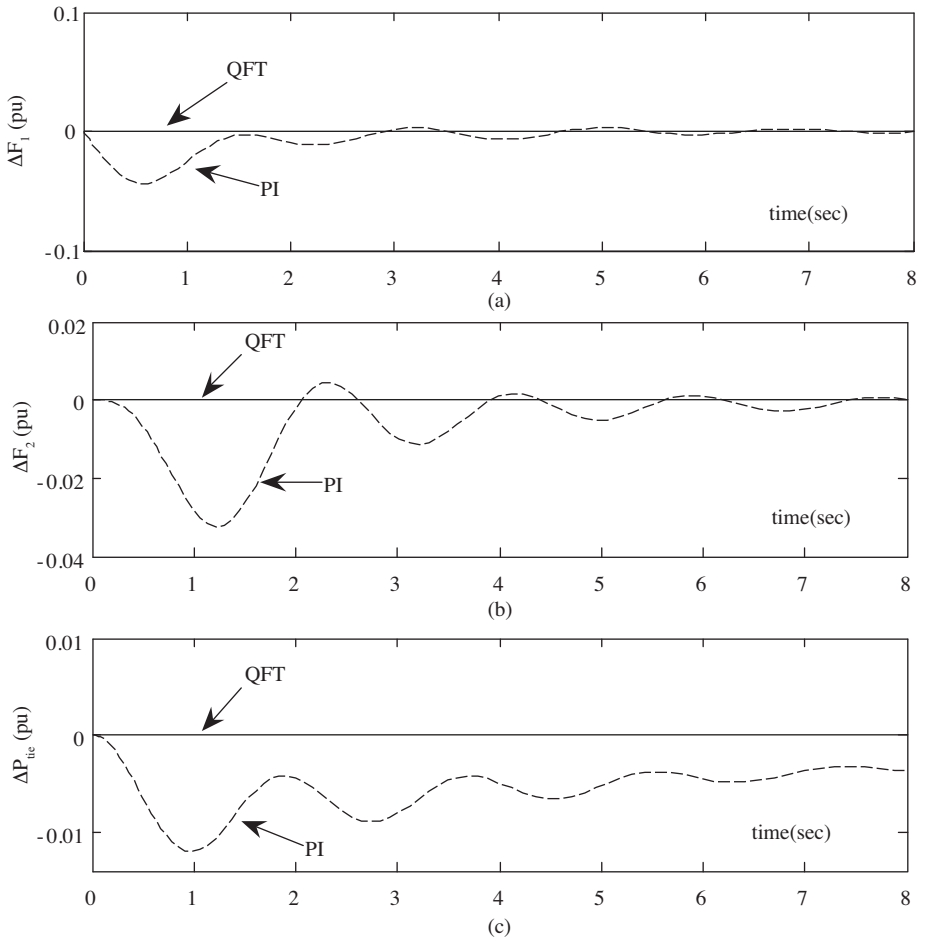

Figure 11. Comparison of two control methods in nominal case for a 2% load step change in first area. For Frequency deviation: $(a)\Delta F_1(t)$, (b) $\Delta F_2(t)$, (c) Tie line power deviation, and $\Delta P_{tie}(t)$.

6. Conclusion

This paper presents the decentralized robust controller design methodology of LFC which is based on Quantitative Feedback Theory. A two-area power system with PI and proposed QFT based controllers has been modeled and simulated. The simulation results show that the responses of QFT controller are significantly better than the conventional GA-PI or PSO-PI controllers. Also, the proposed QFT controllers can present the robust performance. It is shown that the tie line power flow oscillations can be damped by the proposed controller, too.

Appendix A

State space presentation parameters:

T_{ij} Synchronizing coefficient of the tie-line between ith and jth areas

$T_{Ti}i^{th}$ turbine time constant in, seconds

$T_{Gi}i^{th}$ governor time constant in, seconds

$T_{Pi}i^{th}$ subsystem model time constant in, seconds

$K_{Pi}i^{th}$ subsystem gain

R_i Speed regulation for ith subsystem in Hz/p.u. MW

D_ii^{th} load frequency constant

M_ii^{th} Interia constant

ΔP_{tie} Incremental change in the tie-line power

ΔF_ii^{th} area frequency deviation in Hz

$\Delta P_{Di}i^{th}$ area load disturbance in p.u. MW

ΔP_{Ti} Incremental generation change

ΔP_{Gi} Incremental governor valve position change

Appendix B

Nominal parameters of two-area system:

$T_{G1} = T_{G2} = 0.08$ s

$T_{T1} = T_{T2} = 0.3$ s

$T_{P1} = T_{P2} = 20$ s

$K_{P1} = K_{P2} = 120$ Hz/p.u. MW

$R_1 = R_2 = 2.4$ Hz/p.u. MW

$P_r = 2000$ MW (area rated capacity)

$P_{tie\ max} = 200$ MW (tie line capacity)

$T_1 = (P_{tie\ max}/P_r)\ \cos 30^o = 0.0866$ p.u. MW/rad $a_{12} = -1$

Appendix C

$$
\begin{aligned}
S_{11}(j\omega) &= \frac{1 + p_{22}g_2}{(1 + p_{11}g_1)(1 + p_{22}g_2) - p_{12}p_{21}g_1g_2} \\
&= \frac{(p_{22} + g_1 \det P)(1 + p_{22}g_2)}{(p_{22} + g_1 \det P)[(1 + p_{11}g_1)(1 + p_{22}g_2) - p_{12}p_{21}g_1g_2]} \\
&= \frac{\frac{p_{22}(1+g_1p_{11}+p_{22}g_2+g_1g_2 \det P)-g_1p_{12}p_{21}}{[(1+p_{11}g_1)(1+p_{22}g_2)-p_{12}p_{21}g_1g_2]}}{p_{22} + g_1 \det P} \\
&= \frac{p_{22} - p_{12}\frac{p_{21}g_1}{(1+p_{11}g_1)(1+p_{22}g_2)-p_{12}p_{21}g_1g_2}}{p_{22} + g_1 \det P} \\
&= \frac{p_{22} - p_{12}S_{21}}{p_{22} + g_1 \det P}
\end{aligned}
$$

$$
\begin{aligned}
S_{12}(j\omega) &= \frac{-p_{12}g_2}{(1+p_{11}g_1)(1+p_{22}g_2)-p_{12}p_{21}g_1g_2} \\
&= \frac{(p_{22}+g_1\det P)(-p_{12}g_2)}{(p_{22}+g_1\det P)[(1+p_{11}g_1)(1+p_{22}g_2)-p_{12}p_{21}g_1g_2]} \\
&= \frac{\frac{(p_{22}+g_1\det P)(-p_{12}g_2)+(1+p_{11}g_1)(p_{12}-p_{12})}{[(1+p_{11}g_1)(1+p_{22}g_2)-p_{12}p_{21}g_1g_2]}}{p_{22}+g_1\det P} \\
&= \frac{\frac{-p_{12}(1+g_1p_{11}+p_{22}g_2+g_1g_2\det P)+p_{12}(1+p_{11}g_1)}{[(1+p_{11}g_1)(1+p_{22}g_2)-p_{12}p_{21}g_1g_2]}}{p_{22}+g_1\det P} \\
&= \frac{-p_{12}+p_{12}\frac{1+p_{11}g_1}{(1+p_{11}g_1)(1+p_{22}g_2)-p_{12}p_{21}g_1g_2}}{p_{22}+g_1\det P} \\
&= \frac{-p_{12}+p_{12}S_{22}}{p_{22}+g_1\det P}
\end{aligned}
$$

References

[1] P. Kunder, "Power system stability and control" USA, McGrraw-Hill, 1994.

[2] M. Calovic, "Linear regulator design for a load and frequency control theory," IEEE Trans. PAS., Vol. 91, pp. 2271–2285, 1972.

[3] C.F Juang, C.F Lu, "Power system load frequency control by evolutionary fuzzy PI controller", Proc. of IEEE International Conf. on Fuzzy Syst., Vol. 2, , pp. 715–719,Budapest, Hungary, 25-29 July 2004.

[4] C.F Juang, C.F Lu, " Load-frequency control by hybrid evolutionary fuzzy PI controller", IEE Proc. Gener. Transm. Distrib., Vol. 153, No. 2, pp. 196–204, 16 March 2006.

[5] I. Valk, M.Vajta, L. Keviczky, R. Haber, J. Hettessy, "Adaptive load-frequency control of Hungrian power system", Automatica, Vol. 21, pp. 129–137, 1985.

[6] J. Kanniah, S.C. Tripathy, O.P. Malik, G.S.Hope, "Microprocessor-based adaptive load- frequency control", IEE Proc. Part C, Vol. 131, pp. 121–128, 1984.

[7] S.C.Tripathy, P.S. Chandramohanam, R. Balasubramanium, "Self tuning regulator for adaptive load frequency control of power system", The Journal of Institution of Engineers(India), EL79, 103–108, 1998.

[8] C.T.Pan, C. M. liaw "An adaptive controller for power system load frequency control", IEEE Trans. PWRS., Vol. 4 pp. 122–128, 1989.

[9] N.N. Bengamin, W.C. Chan, "Variable structure control of electric power system", IEEE Trans. PAS., Vol. 101, pp. 376–380, 1982

[10] K. Y. Lim, Y Wang, R. Zhou "Robust decentralized load- frequency control of multi-area power systems", IEE Proc. Gener. Transm. Distrb. Vol. 143, No. 5, pp. 377–386, 1996

[11] Y Wang, R. Zhou, C. Wen, "Robust load-frequency controller design for power systems" IEE Proc. Gener. Transm. Distrb. Vol. 140, pp. 11–16, 1993

[12] D. Rerkpreedapong, A. Feliachi, "Robust load frequency control using genetic algorithms and linear matrix inequalities", IEEE Trans. Power Systems, Vol. 18, pp. 855–861, 2003.

[13] A. Kanchanaharuthai, P. Ngamsom, " Robust H_∞ load-frequency control for interconnected power systems with D-stability constraints via LMI approach", Proc. of American Control Conf., Portland, OR, USA, pp. 4387–4392, 2005.

[14] H. Bervani, Y. Mitani, K. Tsuji, "Robust decentralized load-frequency control using an iterative linera matrix inequalities algorithm", IEE Proc. Gener. Transm. Distrb. Vol. 151, No. 3, pp.347–354, 2004.

[15] H. Shayeghi, H.A.Shayanfar, "Application of ANN technique based on μ-synthesis to load-frequency control of interconnected power system", Elsevier, Electrical Power and Energy Systems, Vol. 28, No. 7, pp.503–511, 2006.

[16] C. Borghesani, Y. chait, O. Yaniv, "The QFT frequency domain control design toolbox for use with Matlab, users guide", USA, Terasoft, Inc., 2003.

[17] A. Khodabakhshian, N.Golbon, "Unified PID design for load-frequency control", Proc. of IEEE International Conf. on Control Applic., Vol. 2, pp. 1627- 1632, Taipei, Taiwan, 2004.

[18] A. Khodabakhshian, H. Rahimi, N. Golbon, "QFT design for load frequency control of non-minimum phase hydro power plant", IEEE International Conf. on Control Applics., pp. 1380–1385, Munich, Germany, 2006.

[19] I. Horowitz, "Survey of Quantitative Feedback Theory", Int. J. Nonlinear control, Vol.11, pp. 887–921, 2001.

[20] Shu-Fan Wu, M. J. Grimble, Wei Wei "QFT based robust/fault tolerant flight control design for a remote pilotless vehicle", IEEE transactions on control systems technology, Vol. 8, No. 6, pp. 1010–1016, 2000

[21] W.H. Chen, D.J. Balance, "QFT design for uncertain non-minimum phase and unstable plants revisited", Int. J. Control, Vol. 74, No. 9, pp. 957–965, 2001.

[22] Y. Wang, R. Zhou, C. Wen, "New robust adaptive load-frequency control with system parametric uncertainties", IEE Proc. Gener. Transm. Distrb. Vol. 141, No. 3, pp. 184–190. 1994.

[23] O. Yaniv, "Quantitative feedback design of linear and nonlinear control systems", USA, Kluwer Academic, 1999.

[24] Y. L. Abdel-Magid, M.M. Dawoud, "Genetic algorithms applications in load frequency control", First International Conf. on Genetic Algorithms in Eng. Syst. , Conf. Pub. No. 414 , pp. 207–213, , Sheffield, UK, 1995.

[25] A. Sakhavati, G.B. Gharehpetian, S.H. Hosseini, G. Zarei, S. Shojayee "Load-frequency improvement controller for two area power systems using a novel approach based on genetic algorithm", Proc. of 22^{nd} International Power system Conf., PSC-2007, Tehran, Iran, 19–21, Nov. 2007.

[26] A. Sakhavati, G. B. Gharehpetian, S.H. Hosseini "Decentralized power system Load-frequency control using a novel cost function based on particle swarm optimization", Proc. of 4^{th} International Conf. on Technical and Physical Problems of Power Engineering, TPE2008, Pitesti, Romania. 2008